Available online at www.sciencedirect.com
SCIENCE DIRECT®
Thermochimica Acta 407 (2003) 61–71
thermochimica acta
www.elsevier.com/locate/tca

Temperature-programmed desorption/decomposition with simultaneous DRIFTS analysis: adsorbed pyridine on sulfated ZrO_2 and Pt-promoted sulfated ZrO_2

Robert W. Stevens Jr.[a], Steven S.C. Chuang[a,*], Burtron H. Davis[b]

[a] *Department of Chemical Engineering, The University of Akron, Akron, OH 44325-3906, USA*
[b] *Center for Applied Energy Research, University of Kentucky, Lexington, KY 40511, USA*

Received 18 January 2003; received in revised form 7 May 2003; accepted 8 May 2003

Abstract

The thermal stability and reactivity of adsorbed pyridine on sulfated zirconia and Pt/sulfated zirconia were studied by temperature-programmed desorption (TPD) coupled with infrared spectroscopic and mass spectrometric analyses. Adsorption of pyridine on sulfated zirconia produced two types of adsorbed species: a pyridinium ion on the Brønsted acid site (Pyr-B) giving rise to infrared bands at 1638, 1611, 1486, and 1540 cm^{-1} and a covalently bound species on Lewis acid sites (Pyr-L), giving characteristic bands at 1486 and 1445 cm^{-1} at the same rate, accompanied by the desorption of sulfates to produce gaseous SO_3. TPD studies showed that Pyr-L nearly completely decomposed to CO_2 at 773–823 K, whereas more than 60% Pyr-B remained on the surface in the same temperature range, indicating that Pyr-B possesses higher thermal stability than Pyr-L. The addition of Pt to sulfated zirconia lowers the decomposition temperature of sulfate as SO_2. The study shows that that temperature-programmed desorption/decomposition with simultaneous infrared spectroscopic and mass spectrometric analyses is an effective approach for identifying the structure of the adsorbed species leading to decomposed products. TPD of adsorbed pyridine is not a reliable approach for measuring acid strength of the acid/base catalysts.

Keywords: Sulfated zironia; Pt-promoted sulfated zirconia; Temperature-programmed desorption; Temperature-programmed decomposition; TPD; Adsorption; Dynamics; In situ; Infrared spectroscopy; IR; Diffuse reflectance Fourier transform infrared spectroscopy; DRIFTS; Mass spectrometry

1. Introduction

Temperature-programmed desorption (TPD) and decomposition is an approach for determining the thermal stability and properties of a compound. The approach typically involves heating of the sample at a controlled rate and continuous measurement of change in the property of the compound by monitoring weight changes and evolution of the gaseous species [1–3].

In heterogeneous catalysis research, temperature-programmed desorption/decomposition technique has been widely used to characterize the nature of adsorbed species on the catalysts, reaction pathways, and the acidity/basicity of the oxides [4,5]. Development of a low cost residual gas analyzer or mass spectrometer (MS) has allowed determination of desorption/decomposition profiles of multiple species by

* Corresponding author. Tel.: +1-330-972-6993; fax: +1-330-972-5856.
E-mail address: schuang@uakron.edu (S.S.C. Chuang).

0040-6031/$ – see front matter © 2003 Elsevier B.V. All rights reserved.
doi:10.1016/S0040-6031(03)00305-8

monitoring the composition of the evolving gases from either the decomposition or desorption of the sample. This information obtained from MS measurement has been used (i) to determine adsorption energetics of small molecules such as H_2, (ii) to elucidate the nature of adsorbed species and catalyst surface, and (iii) to postulate the chemical identity of adsorbed species and their reaction pathways occurring during the TPD process. Although postulations derived from TPD study can assist in the understanding of catalysis as well as catalyst development, they could lead to confusion and controversy.

Direct measurement of the surface species during the TPD will provide the chemical identity of adsorbed species leading the desorption and decomposition profiles—direct evidence for elucidation of reaction pathways and catalytic properties. Infrared (IR) spectroscopy is one of the few techniques that allow in situ observation of adsorbed species under reaction conditions. Although TPD and IR have been extensively used in catalyst characterization, simultaneous use of these two techniques are rarely reported [5,6].

We developed a technique involving in situ IR combined with MS to study changes in adsorbate and variation in gas-phase composition during the catalytic reaction [7]. This technique has been applied to monitoring the change in material properties and the evolving gas during the transient condition in which the step and pulse changes in the reactant concentration were applied to the catalytic reactor system [8–10]. We have recently employed this technique to investigate temperature-programmed desorption of adsorbed pyridine on sulfated ZrO_2 (SZ) [11]. Our interest in the SZ catalysts stems from (i) its unique activity for isomerization of alkenes at low temperature [12–14] and (ii) the oxidative properties of SZ exhibited during TPD of benzene and pyridine [15–18]. The latter is reflected in the observation of CO_2 accompanied by the release of SO_2.

It has been well established that pyridine adsorption onto the SZ and Pt/SZ catalysts produces two types of adsorbed species: a pyridinium ion on the Brønsted acid site (Pyr-B) giving rise to infrared bands at 1638, 1611, 1486, and 1540 cm^{-1} and a covalently bound species on Lewis acid sites (Pyr-L), giving characteristic bands at 1486 and 1445 cm^{-1} [19–23]. A key question that remains to be addressed is the role of pyridinium ions and covalently bound pyridine during temperature-programmed desorption/decomposition. In this paper, we studied the interaction between pyridine and SZ and Pt-SZ by TPD approach coupled with MS and IR. IR allows us to observe the surface interaction between adsorbed pyridine and sulfate during TPD. Combining IR with MS not only allow in situ observation of pyridine adsorption dynamics but also greatly enhance the capability of the TPD technique for determining reaction pathway, the nature of adsorbed species, and catalyst surface states; this improved approach allows us to draw an unambiguous conclusion on the role of Pyr-B and Pyr-L in the formation of CO_2 and SO_2. This study reveals advantages of the TPD coupled with MS and IR and its potential for application in thermoanalytical studies.

2. Experimental

2.1. Catalyst preparation

Preparation of ZrO_2 involves: (i) precipitation of zirconium hydroxide by mixing a 0.3 M aqueous solution of $ZrCl_4$ with an excess amount of ammonium hydroxide at a pH of 10.5 and (ii) drying the precipitate at 383 K for 50 h. The dried ZrO_2 was sulfated by immersing it into 0.5 M H_2SO_4 (15 cm^3/g of ZrO_2) and stirred for 2 h. $PtSO_4^{2-}/ZrO_2$ was prepared by impregnating the SO_4^{2-}/ZrO_2 solid with a solution of $H_2PtCl_6{\cdot}6H_2O$ in deionized water. The resulting samples (both SZ and Pt-SZ) were calcined in air at 873 K for 2 h and stored.

Total sulfur content was determined to be 3.18 and 3.43%, respectively, for SZ and 4% Pt/SZ by a Leco SC432 instrument. BET surface area of the two samples, SZ and 4% Pt/SZ was determined to be 139 and 123 m^2/g, respectively.

2.2. Experimental apparatus

The experimental apparatus, shown in Fig. 1, consists of three sections: (i) a gas metering section, (ii) a reactor section, and (iii) an effluent gas analysis section. The gas metering section consists of mass flow controllers (Brooks 5850; not shown), which are used to deliver controlled gas flows to the reactor system, as well as a pyridine saturator. He flow was directed

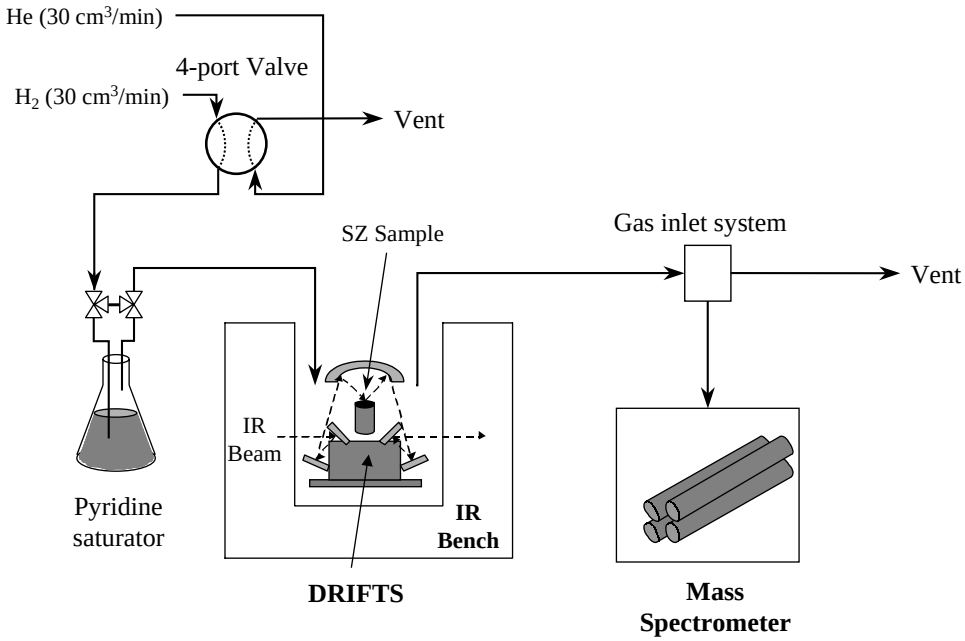

Fig. 1. Schematic of experimental apparatus.

into the saturator through a pair of interconnected three-way valves, delivering a gaseous flow of pyridine (room temperature, partial pressure ≈28 mmHg) to the reactor. The reactor system is made up of an in situ diffuse reflectance infrared Fourier transform spectroscopy (DRIFTS) reactor (Spectra-Tech Inc.) that resides inside an IR bench (Nicolet Magna 550). The effluent section was analyzed via a quadrapole mass spectrometer (Balzers QMG 112). The dynamics of the catalyst surface, its adsorbates, and product formation during the course of the reaction study can be studied with this arrangement.

Seventy five milligrams of sample was used in each experiment and placed into the DRIFTS reactor. Each experiment was analyzed continuously with both IR and MS. The collected IR spectra had a resolution of 4 cm^{-1} and were a result of 32 coadded scans to improve the signal/noise ratio. The catalyst was pretreated in situ by heating the reactor from room temperature to 873 K at a rate of 10 K/min and held for 2 h in a flowing He environment. The reactor was then cooled back to room temperature during which IR spectra of the clean catalyst surface were collected as a function of temperature, hereafter referred to as pretreated backgrounds. The IR bench is a single-beam instrument and therefore it is necessary to collect background spectra (reference spectra) of the catalyst prior to the experiments.

IR data are presented in two formats in this paper: (i) single beam and (ii) absorbance units. Single beam is essentially a plot consisting of background spectra. Single beam is akin to transmittance in the sense that absorbing species are shown in a negative direction; however, it differs from transmittance in that the baseline is curved due to the shape of the IR source spectrum itself (Fig. 2(a)). The second format, absorbance units, uses the background spectra collected following the sample pretreatment; absorbance spectra are calculated from background (prior to experimentation) and sample (during experimentation) spectra of matching temperature. The formula used to calculate absorbance is as follows: $A(\nu) = -\log\{I(\nu)/I_0(\nu)\}$, where $I(\nu)$ and $I_0(\nu)$ refer to IR intensities of the sample and background spectra, respectively, as a function of frequency (wavenumber). Typical spectra of this type are shown in Fig. 3(a). Absorbance spectra relative to the pretreated background gave a clean baseline due to the matched temperatures of the sample/background

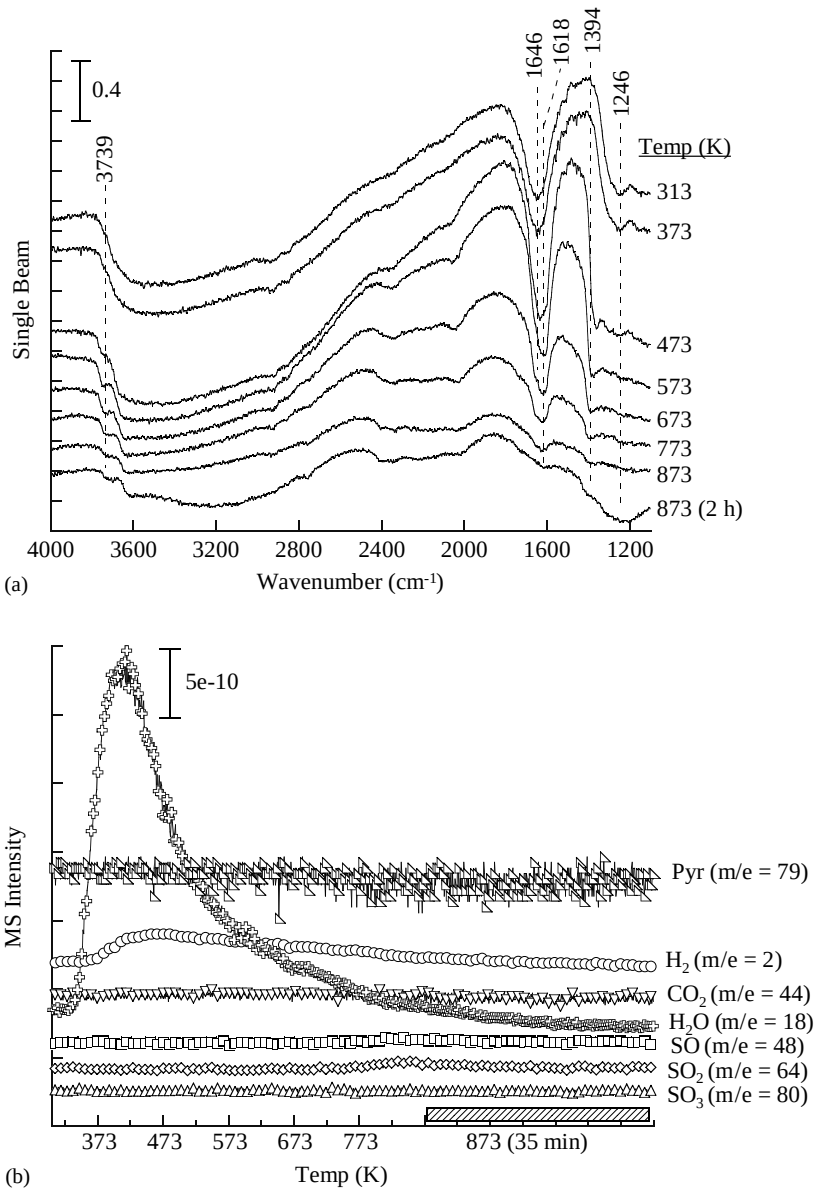

Fig. 2. (a) IR and (b) MS analysis during the pretreatment of SZ from 40 to 600 °C. Background infrared spectra are displayed in (a). The shaded bar on the temperature axis of (b) indicates constant temperature.

spectra and are further rationalized by the fact that the point of reference is a clean surface.

The Balzers QMG 112 mass spectrometer could measure 8 *m*/*e* signals simultaneously; *m*/*e* values of 79, 80, 64, 48, 44, 2, 4, and 18 were monitored corresponding to pyridine, SO_3, SO_2, SO, CO_2, H_2, He, and H_2O, respectively. Total gas flow rates were maintained at 30 cm^3/min throughout all of the experiments.

2.3. Pyridine adsorption (acidity characterization)

Prior to the adsorption of pyridine, the reactor was heated to 423 K. This temperature was selected for the

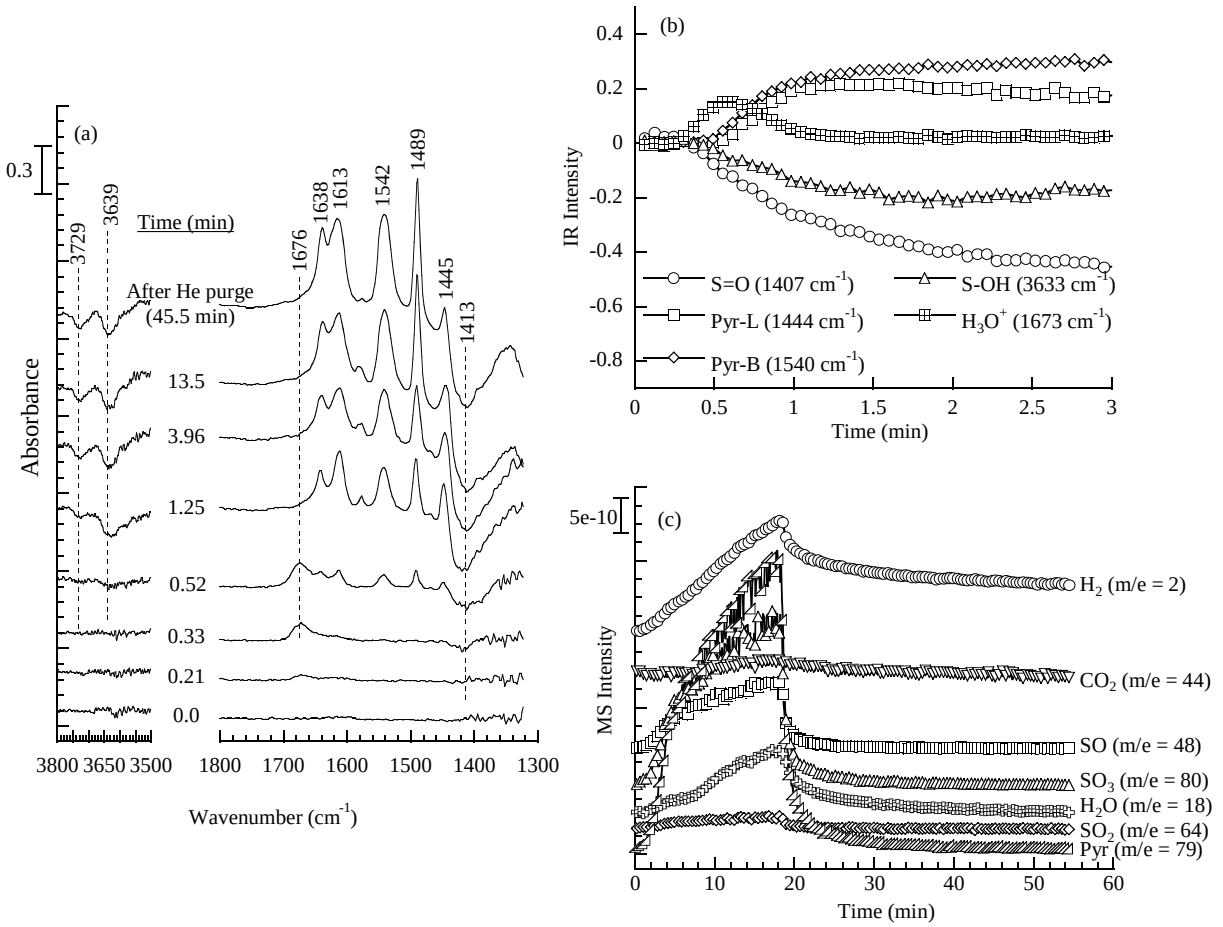

Fig. 3. (a) IR analysis relative to a pretreated background, (b) Peak intensities of selected species, and (c) MS analysis during pyridine adsorption over SZ. Times indicated are relative to the time of pyridine introduction.

ease of comparison with literature data and to insure that pyridine (bp = 389 K) did not condense on the catalyst surface. Gaseous pyridine was sent to the reactor by redirecting the He carrier gas through the pyridine saturator. The SZ sample was exposed to pyridine for about 15 min, during which changes in concentration of adsorbate and gaseous species were recorded via IR and MS. The pyridine/He flow was then replaced by only He in order to remove the weakly bound (physisorbed) pyridine from the surface, leaving only the stronger chemisorbed species, while maintaining the reactor at 423 K until no further changes were observed via IR or MS. Finally, the reactor was cooled to 313 K and a final IR measurement was collected to characterize the pyridine-saturated acid surface.

2.4. Temperature-programmed desorption (TPD)

Following the pyridine adsorption, the reactor was heated at a rate of 10 K/min under He flow from 313 to 873 K. Transient changes to the sample were recorded via IR and MS during the heating profile.

2.5. Hydrogen treatment

The objective of this experiment is to alter the concentration of Brønsted acid sites on the surface, thereby altering the acidity of the surface [12]. This presumes that H_2 addition to the surface of SZ will produce an elevated level of Brønsted acid sites. Furthermore, the addition of Pt as a promoter to the

catalyst should result in an even higher concentration of Brønsted acid sites when combined with the H_2 treatment. The stability of the pyridine complexes to the samples with differing relative levels of Brønsted and Lewis acid sites can be characterized through TPD study.

Separate sets of experiments were conducted with fresh catalysts to examine the effect of H_2 on the Brønsted acidity of the SZ catalysts. After pretreatment and before pyridine adsorption, He flow was replaced by H_2 (30 cm^3/min) with a four-port valve for a period of 15 min at 423 K. The H_2 was then switched back to He and the system was allowed to return to a steady state condition. The remaining stages of the experiment, beginning with pyridine adsorption, were conducted as previously described.

3. Results and discussion

3.1. Pretreatment

Fig. 2 shows the IR spectra of SZ and the MS analysis of the reactor effluent as a function of temperature during the He pretreatment. Upon heating from 313 to 473 K, H_2O and H_2 were evolved (Fig. 2(b)). The difference in the temperatures which yielded a maximum evolution of H_2 and H_2O (456 K versus 408 K) indicates that the H_2 signal is not simply a fragment of H_2O. Furthermore, increasing temperature to 473 K led to the growth of both the H_2O at 1646 cm^{-1} and S=O at 1370–1400 cm^{-1} as well as formation terminal Zr–OH band at 3739 cm^{-1} [24]. Further increase in temperature led to growth of the S=O bond, which shifted to higher frequency as its intensity increases and is ultimately centered at 1394 cm^{-1} as well as a decrease in the broad H_2O band in the 3300–3800 cm^{-1} region. After holding the reactor at a final temperature of 873 K for 2 h, H_2O was completely removed, whereas both terminal OH and S=O became stable at 3739 and 1394 cm^{-1}, respectively. It is important to note that no other species desorbed during the pretreatment of the sample (Fig. 2(b)), indicating that the sulfate groups on the surface of the sample were stable up to at least 873 K. All other samples gave very similar behavior to that depicted in Fig. 2; thus their individual results are not shown.

3.2. Pyridine adsorption

Fig. 3(a) shows absorbance spectra that are relative to a pretreated background during pyridine adsorption at 150 °C. Exposure of the SZ sample to pyridine led to a temporary formation of the 1676 cm^{-1} band which has been assigned to hydronium, H_3O^+ [25]. This species is a precursor for pyridine adsorption. Its disappearance was accompanied by the formation of the pyridinium ion (Brønsted acid site complex; hereafter referred to as "Pyr-B") at 1638, 1613, 1489, and 1542 cm^{-1}, as well as that of covalently bound pyridine (Lewis acid site complex; hereafter referred to as "Pyr-L") at 1489, and 1445 cm^{-1} concurrently with a decrease in S=O at 1413 cm^{-1}.

The variation in the intensity of all the major IR bands with time in Fig. 3(b) was plotted along that of MS intensity in Fig. 3(c) to illustrate the dynamics of pyridine adsorption over SZ. The combined IR and MS observation revealed a number of key features on pyridine adsorption on SZ which was not previously reported. Further pyridine exposure led to (i) increasing intensities of all bands for Pyr-B and Pyr-L, (ii) losses of Zr–OH and S–OH bands 3730 and 3639 cm^{-1}, respectively, (iii) decrease in the S=O band at 1405 cm^{-1} and growth of a broad band in the 1339 cm^{-1} region, and (iv) evolution of H_2O, H_2, and SO_x (Fig. 3(c)). Comparison of the MS fragments of SO_3, SO_2, and SO suggests that the major sulfur species evolved is SO_3.

Pyr-B and Pyr-L changed at the same rate, as shown in Fig. 3(b), suggesting that adsorption of pyridine on Brønsted and Lewis sites occurred at the same rate. It is interesting to note that the intensities of the adsorbed species became constant after 2 min of pyridine exposure, whereas gaseous SO_x, H_2O, and H_2 continued to increase with pyridine as shown in Fig. 3(c). Continuous evolution of SO_x (Fig. 3(c)) without variation of IR profiles (Fig. 3(b)) can be attributed to the fact that the upper portion of the sample, which is analyzed by the DRIFTS, has been saturated with adsorbed pyridine while the remaining sample continues to uptake pyridine as well as desorb SO_x. Upon switching from pyridine to He, the SO_x, H_2O, and H_2 immediately decreased.

The decrease in the S=O stretch can be attributed to a loss of sulfate species (i.e. displaced pyridine adsorption, as evidenced by the formation of SO_3 (Fig. 3(c)) and/or to an interaction between sulfate and pyridine

resulting in a change to the double bond character of S=O [26]. The losses of Zr–OH and S–OH coupled with the formation of the Pyr-B complex band at 1540 cm^{-1} shows that both of these species may serve as Brønsted acid sites according to the following scheme:

$$–OH + Pyr \rightarrow –O^{-} + {}^{+}H\text{-}Pyr$$

The loss intensity of S–OH is greater than that of Zr–OH, suggesting that S–OH is a more significant Brønsted acid site. Pyridine adsorption over the Pt-promoted SZ sample (Pt/SZ) follows the same trends as those reported above. Hence, individual results of pyridine adsorption over Pt/SZ are not shown.

3.3. Hydrogen treatment

Fig. 4 illustrates IR spectra following the H_2 treatment of both SZ and 4% Pt/SZ, relative to a pretreated background, at 423 K. In both cases, formation of bridged OH on Zr (3650–3700 cm^{-1}), adsorbed H_2O (1600–1620 cm^{-1}), and a loss of S=O (1370–1430 cm^{-1}) was observed. No SO_x species were observed to desorb via MS (not shown), thus the decrease in S=O intensity is not due to displacement of SO_x from the SZ surface. It also should be noted that the absence of both terminal OH and S–OH, which would be observed at approximately 3730 and 3630 cm^{-1}, respectively, does not indicate that these species were not present. It simply means that the concentration of these species did not change. The formation of the terminal OH is clearly seen during the pretreatment in Fig. 2. The 4% Pt/SZ sample exhibited a slightly larger loss of S=O as compared to unpromoted SZ. Although the intensity of these various species depends on the Pt loading, the wavenumber of these species, which reflects their nature, remained unchanged. These results suggest that the presence of Pt does not alter the surface chemistry upon H_2 exposure.

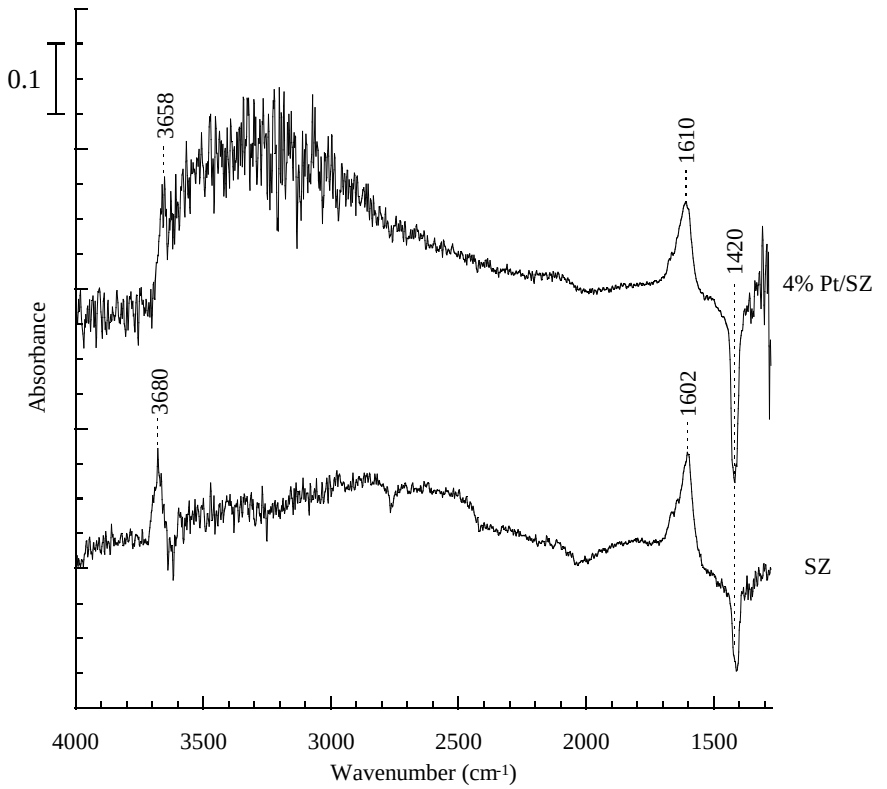

Fig. 4. Comparison of IR spectra, relative to a pretreated sample background, of H_2-treated samples following He flushing.

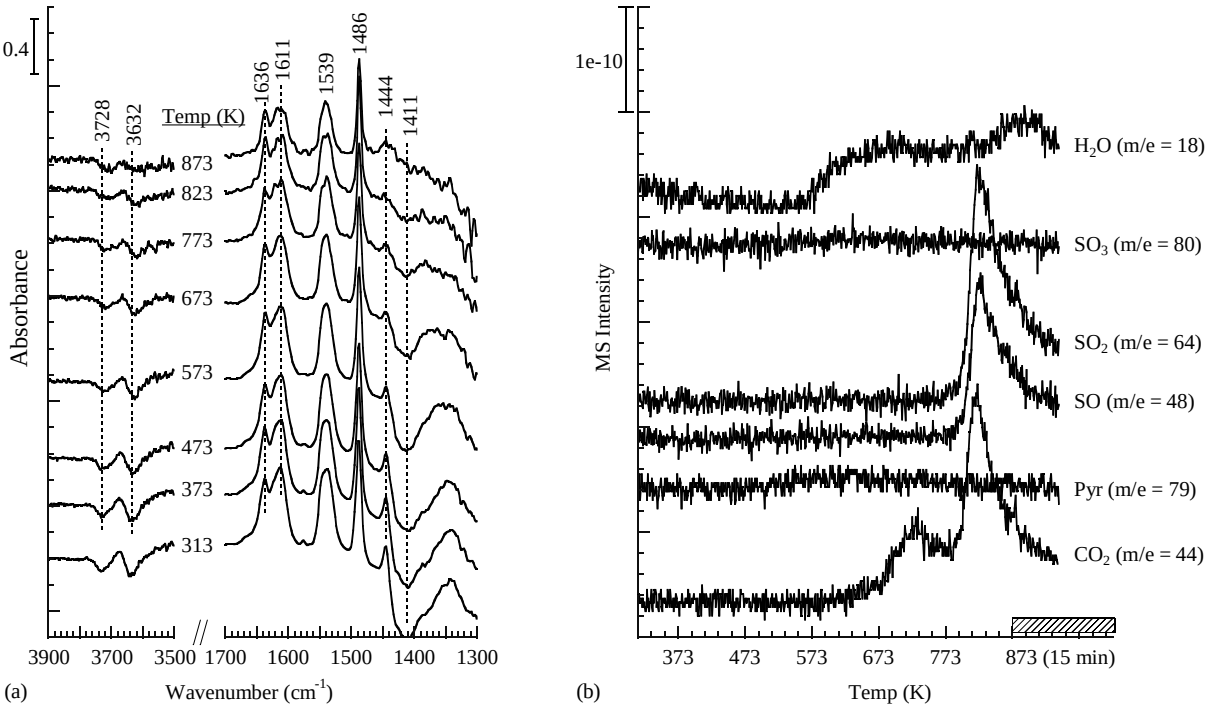

Fig. 5. (a) IR relative to a pretreated sample background and (b) MS analysis during the pyridine TPD from 40 to 600 °C over SZ. The rate of heating used was 10 °C/min.

3.4. Pyridine TPD

Fig. 5 show the IR and MS analyses as a function of temperature during the TPD from 40 to 873 K over SZ catalyst. Increasing temperature from 313 to 573 K resulted in a slight depletion of Zr–OH at 3729 cm^{-1}, S–OH at 3638 cm^{-1} [24], and Pyr-L at both 1575 and 1445 cm^{-1} (Fig. 5(a)), and was accompanied by evolution of H_2O in the reactor effluent (Fig. 5(b)). Increasing the temperature further from 573 to 773 K resulted in a decreasing of all IR intensities and evolution of CO_2. No pyridine desorbed throughout the experiment as indicated by the flat $m/e = 79$ profile of Fig. 5(b). Part of adsorbed pyridine is oxidized to CO_2, indicating that pyridine TPD is not a valid method to gauge acid strength. Further heating from 773 to 873 K resulted in decomposition of the sulfate group as indicated by the SO_2 and SO profiles, evolution of a second, larger CO_2 peak at 813 K and decreases in the intensities of S=O, Zr–OH, and S–OH. Furthermore, Pyr-L at 1444 cm^{-1} is essentially completely removed at 823 K; at 873 K it appears that Pyr-L has returned. It is believed that this returning peak at 1444 cm^{-1} is not Pyr-L but rather a result of the surface rearrangement due to sulfate decomposition. The return of the S=O band at 1411 cm^{-1} (becomes less negative) is quite noteworthy. Recall that the exposure of the SZ catalyst to pyridine resulted in the loss of S=O (Fig. 3) and this was accompanied by evolution of SO_3. The return of the S=O while pyridine decomposes suggests that its initial loss was not solely due to the decomposition of surface sulfate but rather, at least in part, due to an interaction of the adsorbed pyridine with the sulfate group resulting in a change to its chemical bonding (i.e. double bond to single bond).

Fig. 6 depicts similar IR and MS analyses during the TPD over H_2-treated 4% Pt-SZ from 313 to 873 K in He flow. Increasing temperature resulted in the same trends to the adsorbed Pyr-B and Pyr-L as those in Fig. 5, however, there are notable differences: (i) the loss of S=O is not completely restored, (ii) Zr–OH

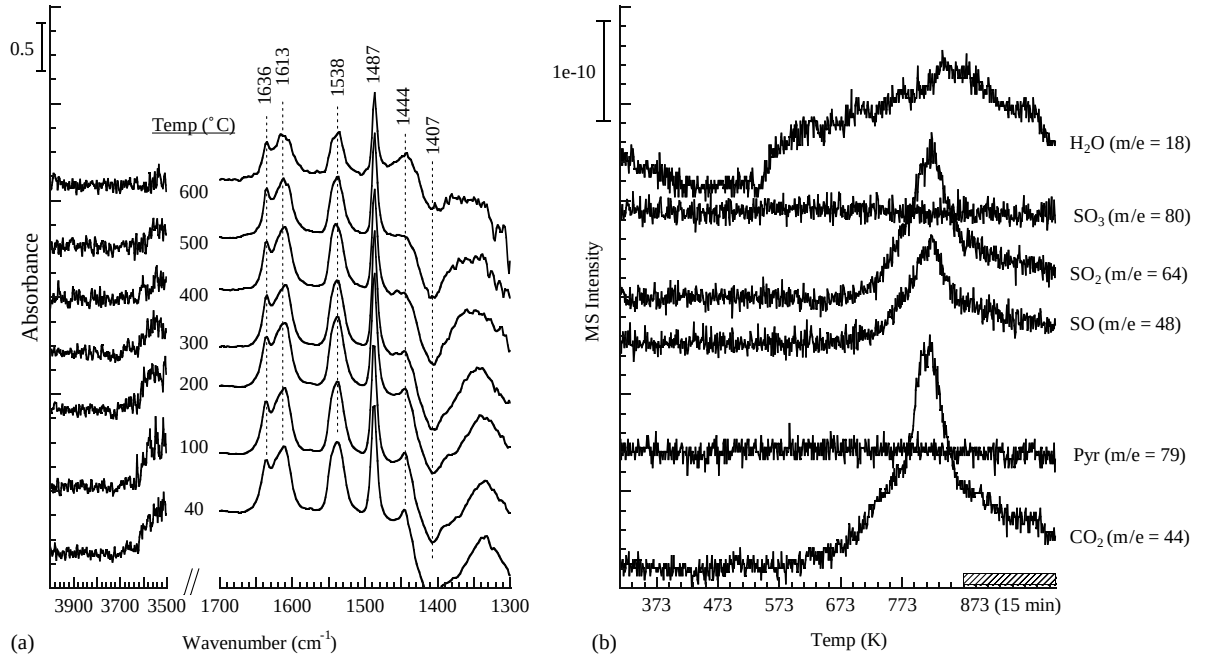

Fig. 6. (a) IR relative to a pretreated sample background and (b) MS analyses during the pyridine TPD from 40 to 600 °C over H_2-treated 4% Pt/SZ. The rate of heating used was 10 °C/min.

and S–OH exhibited no changes over the course of the temperature range studied, and (iii) the CO_2 desorption peak (Fig. 6(b)) is one single peak with a maximum at about 823 K rather the than two peaks shown in Fig. 5. These differences can be due to either the H_2 treatment, Pt promotion, or a combination of both. The individual effects of H_2 and Pt can be seen in Fig. 7.

Fig. 7 depicts a summary of both MS and IR analyses of pyridine TPD over (a) SZ, (b) H_2-treated SZ, (c) 4% Pt/SZ, and (d) H_2-treated 4% Pt/SZ. IR intensities have been normalized in order to clearly illustrate trend information as well as to ease comparison of the data from the separate experiments. This summary highlights a number of key features: (i) the intensity of Pyr-B decreased only slightly at temperatures below 873 K throughout all of the runs, suggesting that it is a relatively stable species, (ii) Pyr-L decreased steadily with the increase in temperature from 313 to 773 K; at 773 K, Pyr-L appeared to decompose to yield CO_2, and (iii) S=O character of the surface increased steadily with temperature while Pyr-L and Pyr-B decreased, indicating that the initial loss of S=O during pyridine adsorption cannot be attributed solely to sulfate displacement, which led to the formation of SO_3. The recovery of S=O appears to be a result of the decomposition of Pyr-L.

The similarity between the IR/MS profiles of Fig. 7(a) and (b) as well as between Fig 7(c) and (d) suggest that H_2 treatment has no effect on the chemistry of the pyridine–SZ interactions. In contrast, comparing the TPD profile of Pt/SZ in Fig. 7(c) and (d) to that of SZ in Fig. 7(a) and (b) clearly demonstrates that Pt led to instability to the sulfate groups of the surface as shown by the lower evolution temperature of SO_2 (673 K versus 793 K). This is complemented by a continuous evolution of CO_2, as opposed to two distinct decomposition peaks. Prior to 773 K, the evolution of CO_2 appears to correspond to the decrease in Pyr-L and it is thus believed that the CO_2 initially comes from oxidation of the pyridine-Lewis complex. Following 773 K, the sulfate group decomposed and it becomes difficult to deduce the surface chemistry.

Decomposition of adsorbed pyridine and sulfates makes pyridine TPD an unreliable tool for gauging the

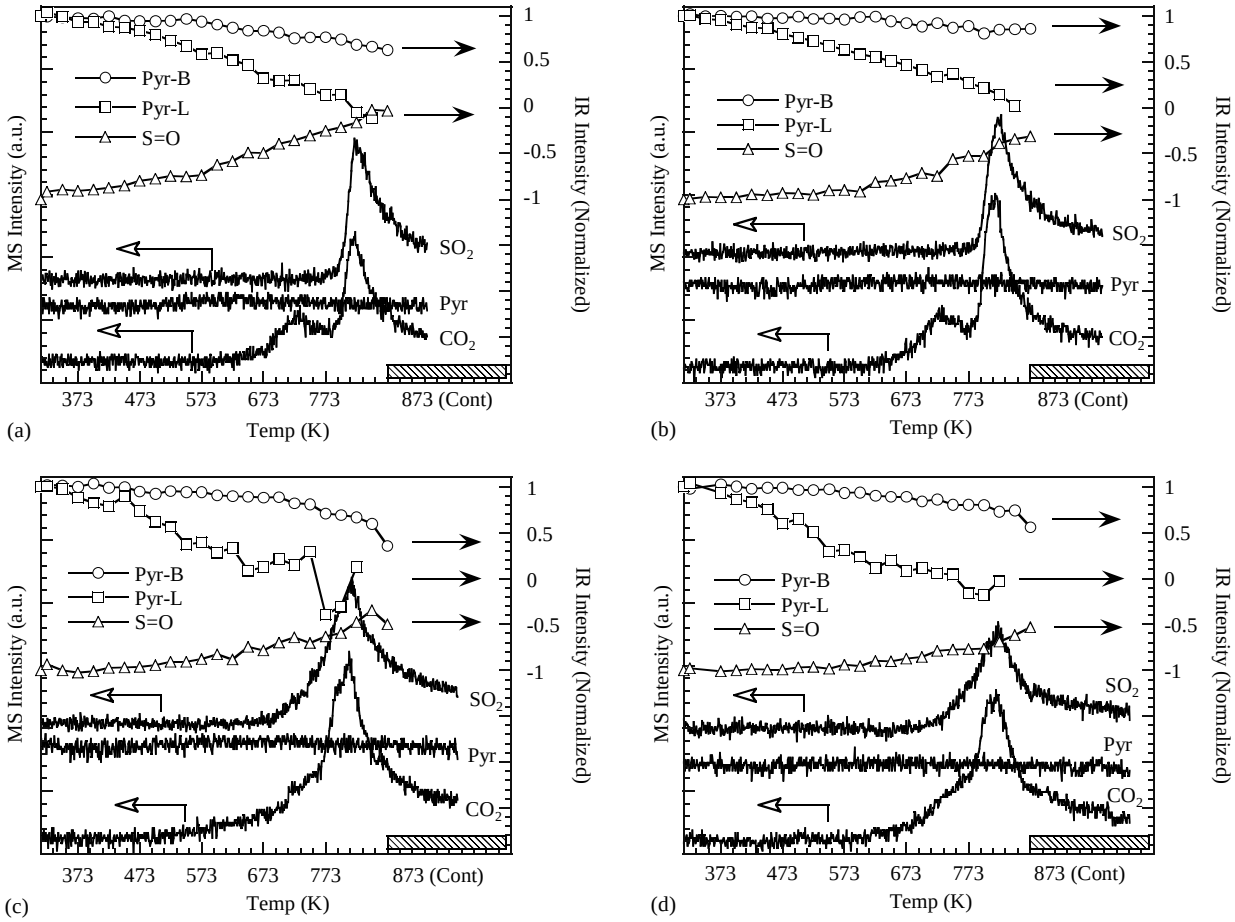

Fig. 7. Pyridine TPD summary. Mass spectral and infrared analyses of selected species showing compositional changes in surface adsorbates and the gaseous effluent as a function of temperature over (a) SZ, (b) H_2-treated SZ, (c) 4% Pt/SZ, and (d) H_2-treated 4% Pt/SZ.

acid strength of the acid/base catalysts. The difference in the sulfate concentration before and after pyridine adsorption makes the correlation between the catalytic reaction rate data and the Lewis to Brønsted acid sites ratio dubious. We recommend that desorption behavior of probe molecules be closely monitored with multiple techniques such as mass and infrared spectroscopy before being applied to probing the properties of a material.

4. Conclusion

Combined IR with MS analysis shows that pyridine adsorption produced Pyr-B and Pyr-L at the same rate, led to suppression of S=O band at 1413 cm^{-1} and desorption of sulfate as SO_3.

Simultaneous measurement of adsorbed species and gaseous species evolved from SZ and Pt/SZ surfaces during TPD shows Pyr-L nearly completely decomposed to CO_2 at 773–823 K; more than 60% Pyr-B remained on the surface in the same temperature range. Pyr-B exhibited higher thermal stability than Pyr-L. No major difference in the behavior of Pyr-B and Pyr-L was observed on SZ and Pt/SZ. The major effect of Pt is to promote the desorption of sulfate as SO_2. The study demonstrates that temperature-programmed desorption/decomposition with simultaneous analysis is an effective approach in identifying the structure of the adsorbed species leading to decomposed products.

Acknowledgements

This work was partially financed by the Ohio Board of Regents Grant R4552-OBR.

References

[1] J.L. Falconer, J.A. Schwarz, Catal. Rev.-Sci. Eng. 25 (1983) 141.
[2] R.J. Cvetanovic, Y. Amenomiya, Catal. Rev. 6 (1972) 21.
[3] S.A. Hedrick, S.S.C. Chuang, Thermochim. Acta 315 (1998) 159.
[4] R.J. Gorte, Catal. Today 28 (1996) 405.
[5] R. Krishnamurthy, S.S.C. Chuang, Thermochim. Acta 262 (1995) 215.
[6] Y. Chi, S.S.C. Chuang, J. Phys. Chem. B 104 (2000) 4673.
[7] S.S.C. Chuang, M.A. Brundage, M.W. Balakos, G. Srinivas, Appl. Spectrosc. 49 (1995) 1151.
[8] S.S.C. Chuang, M.A. Brundage, M.W. Balakos, Appl. Catal. A 151 (1997) 333.
[9] Y. Chi, S.S.C. Chuang, Catal. Today 62 (2000) 303.
[10] M.V. Konduru, S.S.C. Chuang, X. Kang, J. Phys. Chem. B 105 (2001) 10918.
[11] R.W. Stevens Jr., S.S.C. Chuang, Appl. Catal. A, in press.
[12] X. Song, A. Sayari, Catal. Rev.-Sci. Eng. 38 (1996) 329.
[13] B.Q. Xu, W.M.H. Sachtler, J. Catal. 165 (1997) 231.
[14] S. Hammache, J.G. Goodwin Jr, J. Catal. 211 (2002) 316.
[15] K.T. Wan, C.B. Khouw, M.E. Davis, J. Catal. 158 (1996) 311.
[16] E.C. Sikabwe, M.A. Coelho, D.E. Resasco, R.L. White, Catal. Lett. 34 (1995) 23.
[17] A. Jatia, C. Chang, J.D. MacLeod, T. Okubo, M.E. Davis, Catal. Lett. 25 (1994) 21.
[18] W.M. Hua, C.X. Miao, J.M. Chen, Z. Gao, Mater. Chem. Phys. 45 (1996) 220.
[19] D.J. Zalewski, S. Alerasool, P.K. Doolin, Catal. Today 53 (1999) 419.
[20] T. Yamaguchi, T. Jin, K. Tanabe, J. Phys. Chem. 90 (1986) 3148.
[21] B.H. Davis, R.A. Keogh, S. Alerasool, D.J. Zalewski, D.E. Day, P.K. Doolin, J. Catal. 183 (1999) 45.
[22] C. Zhang, R. Miranda, B.H. Davis, Catal. Lett. 29 (1994) 349.
[23] B. Li, R.D. Gonzalez, Catal. Today 46 (1998) 55.
[24] E.E. Platero, M.P. Mentruit, Catal. Lett. 30 (1995) 31.
[25] F. Babou, G. Coudurier, J.C. Vedrine, J. Catal. 152 (1995) 341.
[26] T. Jin, T. Yamaguchi, K. Tanabe, J. Phys. Chem. 90 (1986) 4794.